Optimizing EPI Image Quality Beyond Linear Phase Corrections with Dual-Polarity GRAPPA

André Fischer, Ph.D.[1]; Wei Liu Ph.D.[1]; Kun Zhou Ph.D.[2]

[1]Siemens Healthineers, Erlangen, Germany
[2]Siemens Shenzhen Magnetic Resonance Ltd., Shenzhen, China

Echo planar imaging (EPI) [1, 2] is one of the fastest methods to acquire magnetic resonance imaging (MRI) data. Therefore, it has been the method of choice to collect imaging data as fast as possible when the desired signal is quickly decaying. Examples include T2*-weighted imaging, functional MRI (fMRI, [3–6]), and diffusion-weighted imaging (DWI, [7–9]) including diffusion tensor imaging (DTI, [10]). EPI is very sensitive to any magnetic field inhomogeneities. While B_0 inhomogeneities can be largely addressed by shimming, the human body introduces inhomogeneities that are difficult to compensate. Susceptibility-induced inhomogeneities exist at any interface between materials where the magnetic susceptibility quickly changes. Examples include air-tissue interfaces, such as the sinuses in the human skull, that result in significant geometric distortions in these areas. A third mechanism for inhomogeneities are eddy currents that result from the rapid switching of gradient coils. Any material of the MRI scanner and within the patient that has a non-vanishing magnetic susceptibility will introduce eddy currents. When designing an MRI system, great care is taken to minimize eddy currents and implement eddy current compensation mechanisms. However, switching the gradient with opposite amplitude typically results in different eddy currents. Since EPI imaging relies on reading adjacent *k*-space lines with reverse readout gradient amplitude. Eddy currents on positive readout polarity (RO+) will be slightly different from eddy currents when reading data with negative polarity (RO-). These differences manifest as Nyquist ghosting, which is caused by phase differences between RO+ and RO- readouts. Nyquist ghosting corrections (NGC) typically employ a linear model to compensate these phase differences. However, it is quite obvious that the combination of B_0 inhomogeneities, the presence of the human body, susceptibility changes, and eddy currents can lead to higher order phase differences that are very difficult to model and compensate.

With the introduction of the MAGNETOM Cima.X[1] the most powerful clinical Siemens Healthineers 3T system will be available. The Gemini gradient coil will enable a gradient performance comparable to MAGNETOM Connectom, which was only designed as a research tool. With MAGNETOM Cima.X, we are planning to make Connectom-like power accessible by the clinical community, enabling to utilize the Human Connectom Project (HCP) protocols and expand even beyond. At the core of the HCP is tractography, which relies on highly diffusion-weighted data acquired in many different diffusion directions. As described above, EPI is at the core of diffusion imaging. Addressing phase errors on MAGNETOM Cima.X to enable the highest quality DWI, DTI, and fMRI was a cornerstone during development, and resulted in the introduction of a new phase correction that is embedded into image reconstruction: dual-polarity GRAPPA (DPG)[1] [12].

DPG is the culmination of several preceding methods that are beyond the scope of this manuscript. However, it is worth mentioning that methods such as ghost elimination via spatial and temporal encoding (GESTE) [13], fast-low angle excitation echo-planar technique (FLEET) [14, 15], and phase labeling for additional coordinate encoding (PLACE) [16] play an instrumental role in designing the latest correction methods. What matters is that DPG is a more powerful technique to address even higher order phase variations in EPI, thereby optimizing in particular high-end diffusion applications in which uncorrected phase variations can have a substantial effect.

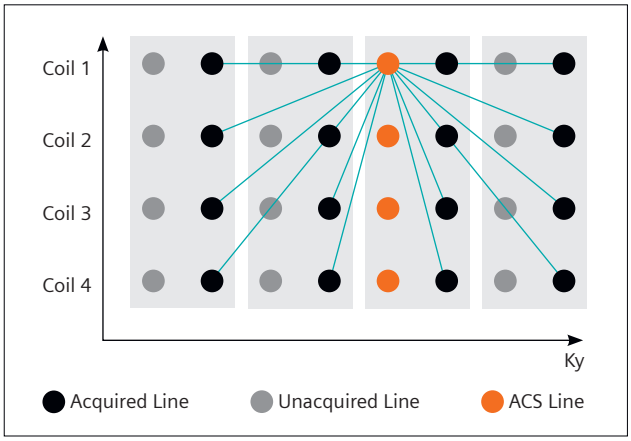

1 GRAPPA kernel calibration

[1]*Work in progress the product is still under development and not commercially available. Its future availability cannot be ensured.*

As the name implies, DPG is based on GRAPPA [17], the standard parallel imaging reconstruction on MRI scanners from Siemens Healthineers. To understand why DPG is so advantageous, it helps to recapitulate GRAPPA.

When parallel imaging came up around the turn of the millennium, the first method published was SENSE [18], which operates in image space. It relies on explicit knowledge of the coil sensitivities of the receiver array. The final reconstruction is a matrix inversion in image space involving the undersampled images and the coil sensitivity profiles. However, determining these coil sensitivity profiles can be challenging, e.g., in areas with low proton density such as the lungs. Due to the nature of the Fourier transform, all methods that can be employed in image space should also have a counterpart in *k*-space, and GRAPPA can be seen as the *k*-space domain counterpart to SENSE. While the underlying principle is the same as for SENSE, GRAPPA does not require explicitly derived coil sensitivity profiles. Instead, it calibrates a convolution kernel, the GRAPPA kernel, on auto-calibration signal (ACS) lines. These ACS lines are a Nyquist-sampled region in *k*-space center, solely used for GRAPPA kernel calibration. Subsequently, the kernel is used to synthesize the missing *k*-space data by convolution with the undersampled *k*-space data.

The ACS lines used for GRAPPA kernel calibration need to be free of artifacts to result in optimal image quality. This poses a real challenge in EPI due to the phase variations described earlier between *k*-space lines acquired with

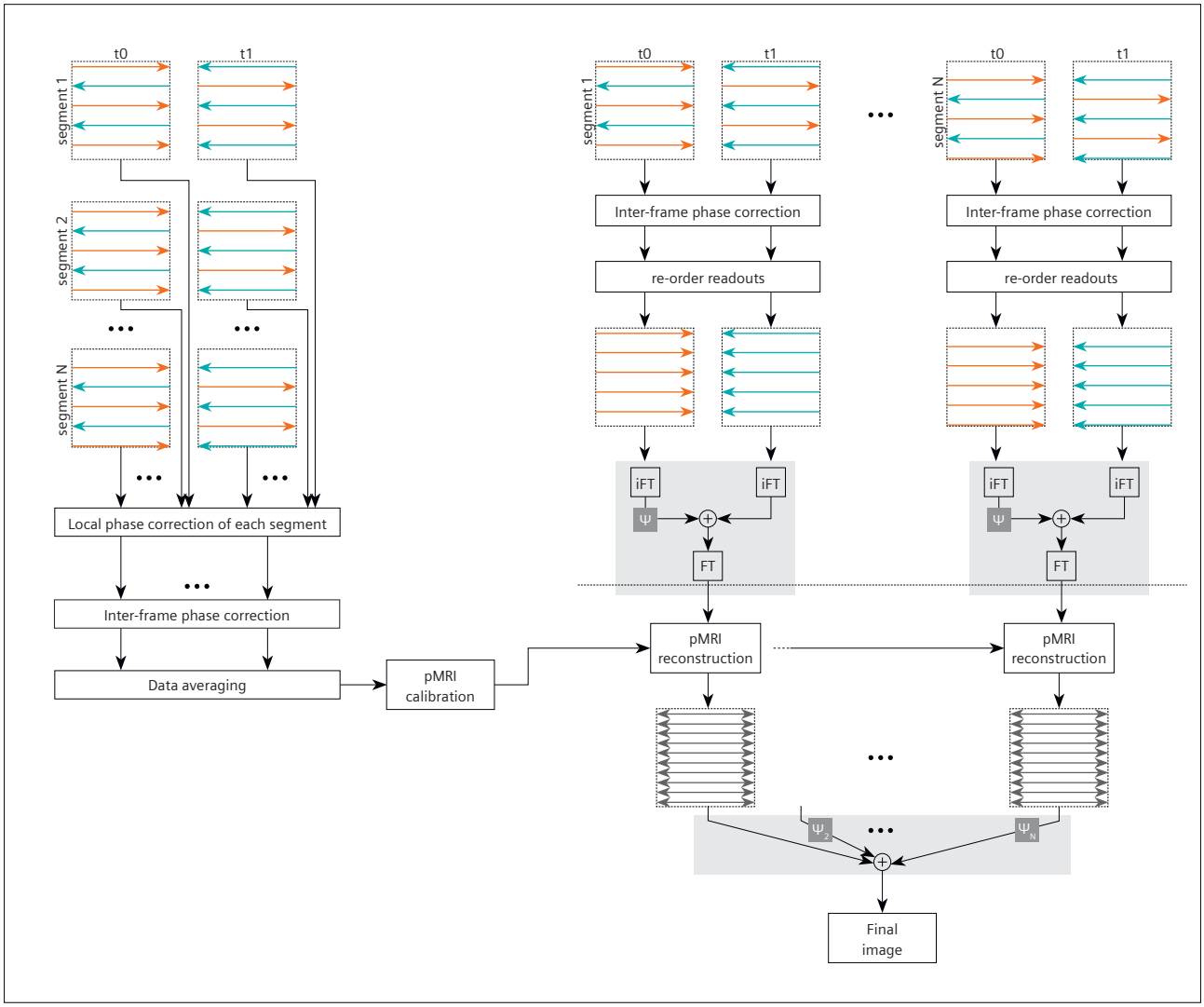

2 Processing for multi-shot EPI calibration data to obtain ghost-free target data for DPG-GRAPPA kernel calibration. Starting on the left side, the FLEET data segments are corrected using LPC, followed by subsequent IFPC. After averaging of these corrected data with PLACE processing, temporary GRAPPA weights are determined for each segment. Moving to the right side, after LPC and IFPC, readouts are reordered such that RO+ and RO- segments emerge. After combination of RO+ and RO- data, the temporary GRAPPA weights determined earlier are applied to reconstruct the missing lines in each segment. Combining these images results in ghost-free target data for DPG calibration.

RO+ and RO- polarity. Consequently, several methods were developed to enable high-quality ACS data to be obtained for GRAPPA kernel calibration. Approaches such as PLACE or GESTE aim to segment and sort the collected data, such that all ACS *k*-space lines were acquired with either RO+ or RO-, but not a mixed readout polarity.

However, those methods alone can't fully compensate all effects. This is, where DPG comes in: As mentioned, a GRAPPA kernel needs to be calibrated. Calibration here refers to solving the following equation:

$$T = wS$$

In this linear equation system, S refers to source data points, T refers to the target data points that we want to reconstruct, and w is the weight set that we typically call the GRAPPA kernel. A pictorial description of this procedure can be found in Figure 1. Please note that all depicted source points from all coil elements of the receiver array are fitted to every single target point in every coil element. The coil readout dimension is omitted in Figure 1 for illustration purposes. In DPG, the source data during calibration consist of two different datasets: RO+ and RO-. These datasets have not been ghosting-corrected so far. However, the calibration target data need to be artifact free, i.e., they need to be ghost-corrected and should not show physiological variations. Obtaining these target data requires a combination of FLEET, GESTE, a local phase correction (LPC) [19], and the aforementioned segmentation and sorting of the acquired ACS data. Details on this can be found in the appendix of the DPG paper [12] and in Figure 2. Please note one small difference compared to Figure 10 from [12]: After the LPC step on the left-hand side and before the readout reordering of the segments on the right-hand side, an additional inter-frame phase correction (IFPC) was applied [20]. This IFPC helped to remove linear phase shifts along the phase encoding direction, thereby removing another potential source of ghosting in the calibration data.

Finally, proper GRAPPA weights can be calibrated, the procedure is explained in Figure 3. Source points from RO+ and RO- are compiled and fitted to a target point of the ghost-free target data. As can be seen, many different GRAPPA kernels can be calibrated using such an approach. One substantial difference to standard GRAPPA is shown in kernels #3–#6: Here, a target point sits in the region of the source points. Why would you want to do this? Keep in mind that the RO+ and RO- source point datasets have not yet been ghost-corrected. Consequently, also *k*-space point locations that lie within the source point region require a reconstruction using DPG to get rid of potential ghosting artifacts in the final reconstructed image.

Once the GRAPPA kernels have been calibrated, the reconstruction procedure is equivalent to standard GRAPPA,

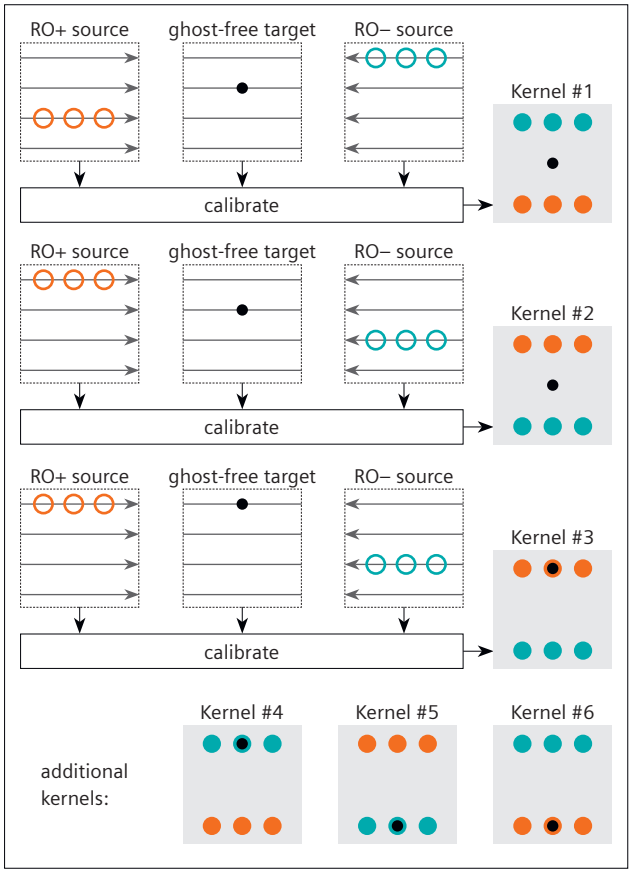

3 Calibration of DPG kernels on exemplary 2 × 3 pattern with R = 2 undersampling

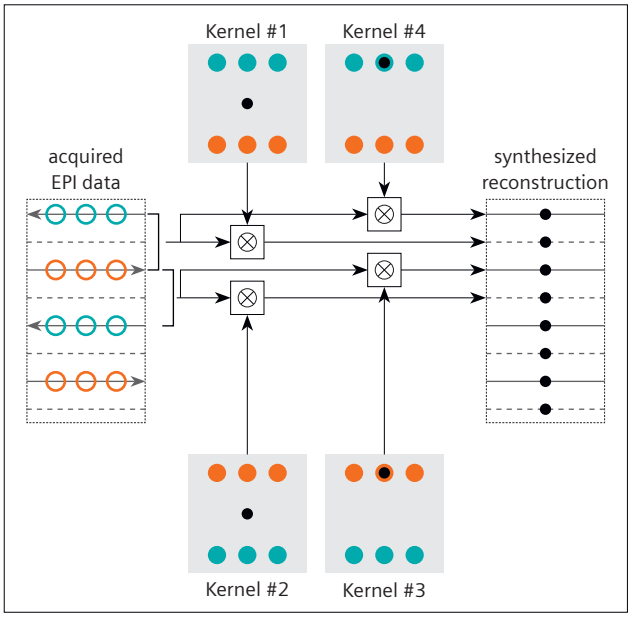

4 Application of calibrated 2 × 3 DPG kernels

except that several kernels have to be used. Depending on the *k*-space location, the corresponding kernel has to be applied to the undersampled *k*-space and ghost-artifact corrected images are the result. This principle is shown in Figure 4 for a R = 2 undersampled single-shot EPI example. Neighboring acquired *k*-space lines have different readout polarity RO+ and RO-, necessitating different kernels to reconstruct missing *k*-space points and ghost-correct the acquired points.

For the clinical user, DPG will be accessible for EPI imaging via a new checkbox on the Sequence > Part 2 card (see Figure 5). The checkbox name is "Ghost reduction" which precisely describes what DPG is doing. Also, a new reference scan is available: FLEET/Separate can be selected on the Resolution > Acceleration card under the "Reference Scan" drop down menu (see Figure 6). These options will be available for MAGNETOM Cima.X[1] and Cima.X Fit[1] with software release *syngo* MR XA61. A final remark on FLEET: This new reference scan minimizes the effects of potential motion within one slice due to different motion states of the acquired segments. This motion can occur if the segments that contribute to the *k*-space of a single slice of reference data are acquired with a large time difference. If motion was present in the reference scan, the GRAPPA weights are suboptimal, resulting in compromised image quality. FLEET can be seen as an additional tool to optimize the quality of the reference scan, but it is not mandatory for use of DPG.

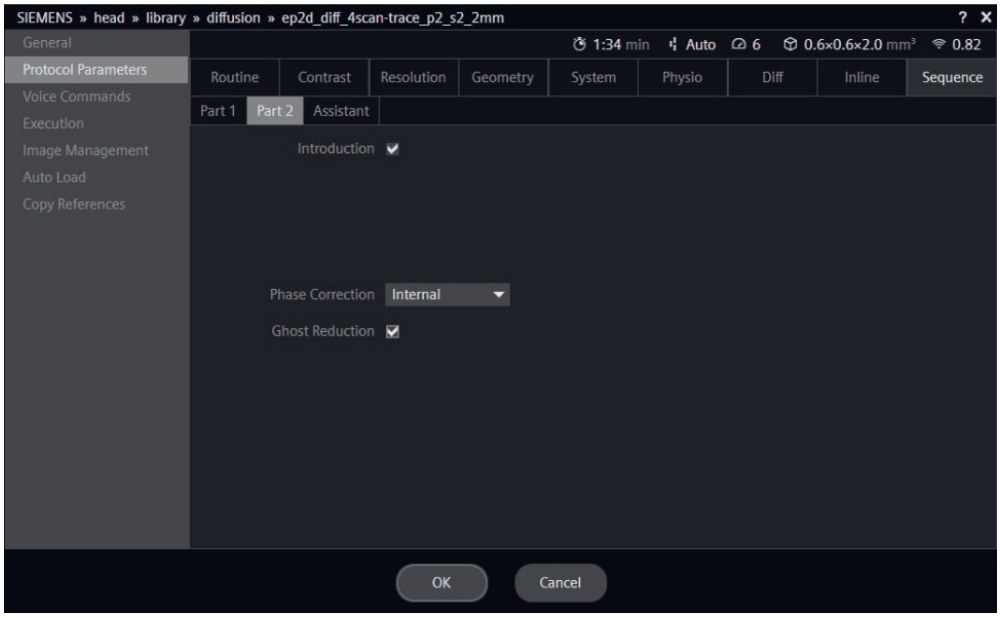

5 Dual-polarity GRAPPA is available when selecting "Ghost Reduction" in the UI and can be found on the Sequence > Part 2 tab

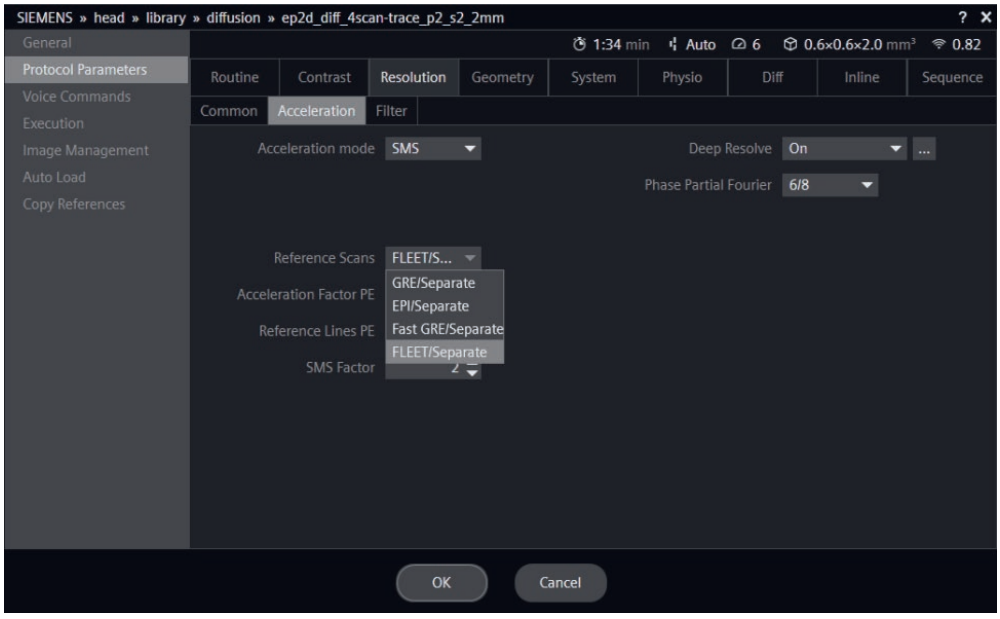

6 The new FLEET reference scan can be selected as usual on the Resolution > Acceleration tab

Figure 7 shows an example of the DPG performance in BOLD imaging for fMRI. If DPG is not used, Nyquist ghosting is visible, here in two locations anterior and posterior of the brain due to the R = 3 acceleration. When using DPG in the image reconstruction pipeline, ghosting artifacts are effectively addressed, resulting in optimal image quality in fMRI.

Figure 8 highlights the benefit of DPG in an example of single-shot EPI DWI where b0 images are shown. The subtle ghosting artifact visible in the right hemisphere of the brain can be eliminated by DPG, resulting in artifact-free DWI datasets. Again, DPG does a really good job in eliminating the ghost.

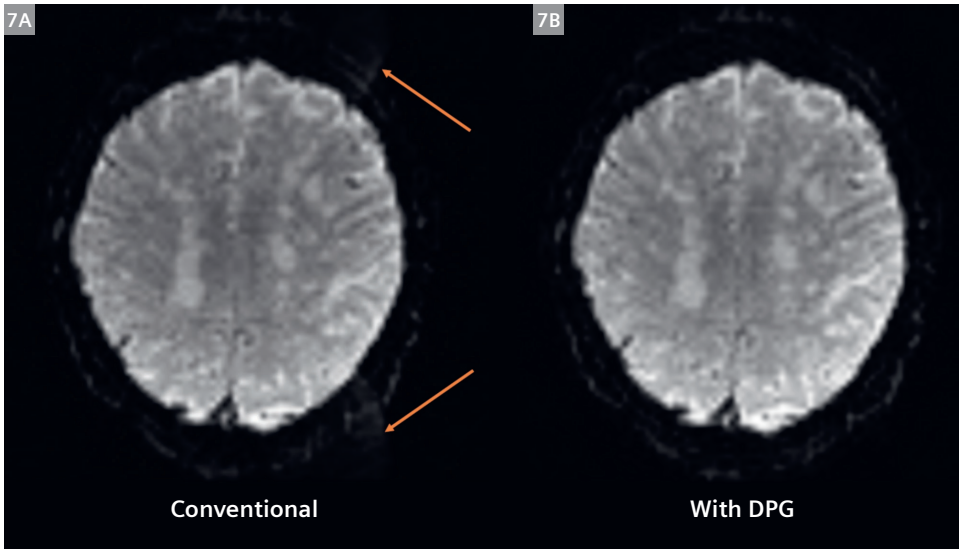

2aaaa2649

7 Effect of Dual-polarity GRAPPA (DPG) in EPI BOLD imaging for fMRI. **(7A)** Ghosting is visible in the anterior and posterior of the brain due to R = 3 undersampling if ghost reduction is turned off. **(7B)** When DPG is turned on, the ghosting is effectively addressed, resulting in clean BOLD images.

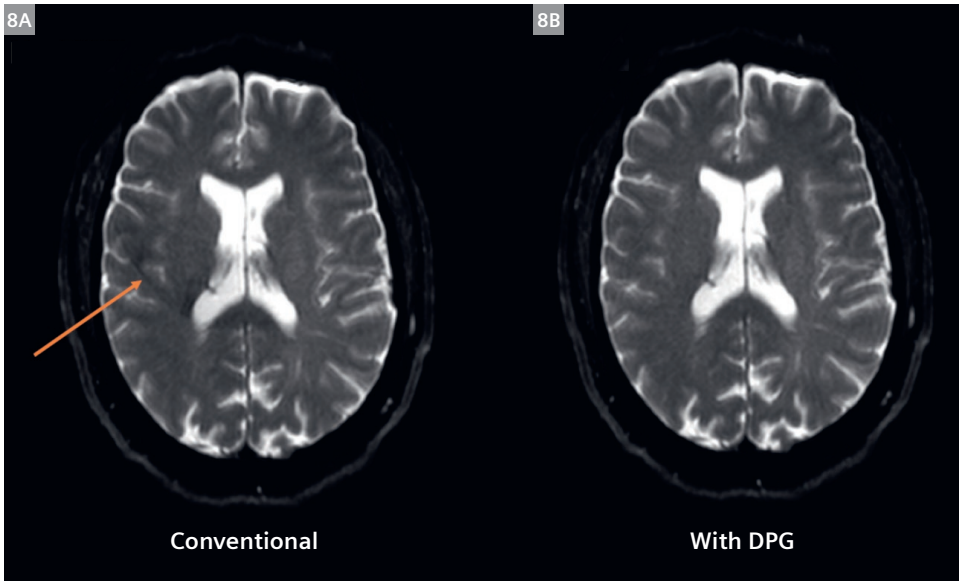

2aaaa2742

8 Effect of Dual-polarity GRAPPA (DPG) in EPI diffusion imaging. **(8A)** Subtle ghosting is visible on the right side of the brain if ghost reduction is turned off. **(8B)** When DPG is turned on, no ghosting is visible anymore.

Conclusion

EPI imaging is a cornerstone for neuro imaging, including DWI, fMRI, and contrast-enhanced perfusion imaging. Beyond neuro, DWI or perfusion imaging in the prostate and in body imaging is of great clinical relevance. In all the mentioned body regions, susceptibility changes as well as eddy currents are additional sources of phase variations next to the B_0 inhomogeneities of the main magnetic field. Proper phase correction is therefore mandatory for meaningful EPI imaging. DPG is the latest addition to established phase correction methods such as LPC, PLACE and GESTE, and DPG can correct higher order phase variations without explicitly determining or modeling these variations. Therefore, DPG will become a standard ghost reduction tool on all MAGNETOM systems operating on *syngo* MR XA60/61 or later to enable optimal EPI imaging in all body areas.

References

1 P. Mansfield. Multi-planar image formation using NMR spin echoes. J Phys C: Solid State Phys, vol. 10, pp. L55-L58, 1977.
2 M. K. Stehling, R. Turner and P. Mansfield. Echo-planar imaging: magnetic resonance imaging in a fraction of a second. Science, vol. 254, pp. 43-50, 1991.
3 S. Ogawa, T. M. Lee, A. R. Kay and D. W. Tank. Brain magnetic resonance imaging with contrast dependent on blood oxygenation. Proc Natl Acad Sci USA, vol. 87, pp. 9868-19872, 1990.
4 P. A. Bandettini, E. C. Wong, R. S. Hinks, R. S. Tikofsky and J. S. Hyde. Time course EPI of human brain function during task activation. Magn Reson Med, vol. 25, pp. 390-397, 1992.
5 K. K. Kwong, J. W. Belliveau, D. A. Chesler, I. E. Goldberg, R. M. Weisskoff, B. P. Poncelet, D. N. Kennedy, E. F. Halpemet and B. R. Rosen. Dynamic magnetic resonance imaging of human brain activity during primary sensory stimulation. Proc Natl Acad Sci USA, vol. 89, pp. 5675-5679, 1992.
6 S. Ogawa, D. W. Tank, R. S. Menon, J. M. Ellermann, S. G. Kim, H. Merkle and K. Ugurbil. Intrinsic Signal Changes Accompanying Sensory Stimulation: Functional Brain Mapping With Magnetic Resonance Imaging. Proc Natl Acad Sci USA, vol. 89, pp. 5951-5955, 1992.
7 E. O. Stejskal and J. E. Tanner. Spin diffusion measurements: spin echoes in the presence of. J Chem Phys, vol. 42, pp. 288-292, 1965.
8 D. Le Bihan and E. Breton. Imagerie de diffusion in-vivo par résonance magnétique. Comptes-Rendus l'Académie des Sci, vol. 93, pp. 27-34, 1985.
9 D. Le Bihan, E. Breton and A. Syrota. In-vivo self-diffusion magnetic resonance imaging. Proc SMRM, vol. 4, pp. 1238-1239, 1985.
10 P. J. Basser, J. Mattiello and D. Le Bihan. Estimation of the effective self-diffusion-tensor. J Magn Reson B, vol. 103, pp. 247-254, 1994.
11 V. M. Runge and J. T. Heverhagen. The Clinical Utility of Magnetic Resonance Imaging According to Field Strength, Specifically Addressing the Breadth of Current State-of-the-Art Systems, Which Include 0.55 T, 1.5 T, 3 T, and 7 T. Invest Radiol, vol. 57, pp. 1-12, 2022.
12 W. S. Hoge and J. R. Polimeni. Dual-polarity GRAPPA for simultaneous reconstruction and ghost correction of EPI data. Magn Reson Med, vol. 76, pp. 32-44, 2016.
13 W. S. Hoge, H. Tan and R. A. Kraft. Robust EPI Nyquist Ghost Elimination via Spatial and Temporal Encoding. Magn Reson Med, vol. 64, pp. 1781-1791, 2010.
14 B. Chapman, R. Turner, R. J. Ordidge, M. Doyle, M. Cawley, R. Coxon, P. Glover and P. Mansfield. Real-Time Movie Imaging from a Single Cardiac Cycle by NMR. Magn Reson Med, vol. 5, pp. 246-254, 1987.
15 J. R. Polimeni, H. Bhat, T. Witzel, T. Brenner, T. Feiweier, S. J. Inati, V. Renvall, K. Heberlein and L. L. Wald. Reducing Sensitivity Losses Due to Respiration and Motion in Accelerated Echo Planar Imaging by Reordering the Autocalibration Data Acquisition. Magn Reson Med, vol. 75, pp. 665-679, 2016.
16 Q. S. Xiang and F. Q. Ye. Correction for Geometric Distortion and N/2 Ghosting in EPI by Phase Labeling for Additional Coordinate Encoding (PLACE). Magn Reson Med, vol. 57, pp. 731-741, 2007.
17 M. A. Griswold, P. M. Jakob, R. M. Heidemann, M. Nittka, V. Jellus, J. Wang, B. Kiefer and A. Haase. Generalized Autocalibrating Partially Parallel Acquisitions (GRAPPA). Magn Reson Med, vol. 47, pp. 1202-1210, 2002.
18 K. P. Pruessmann, M. Weiger, M. B. Scheidegger and P. Boesiger. SENSE: Sensitivity Encoding for Fast MRI. Magn Reson Med, vol. 42, pp. 952-962, 1999.
19 T. Feiweier. Magnetic resonance method and apparatus to determine phase correction parameters. US Patent 8,497,681, July 30, 2013.
20 Y. V. Chang, K. Zhou, W. S. Hoge, U. Hoelscher, W. Liu and J. R. Polimeni. Inter-frame phase alignment for Echo Planar Imaging calibration data acquired with opposite read-out polarities. Proc ISMRM, vol. 27, p. 928, 2019.

Contact

André Fischer, Ph.D.
Global Segment Manager Neurology
Siemens Healthineers
SHS DI MR M&S CSM
Allee am Roethelheimpark 2
91052 Erlangen, Germany
andre.fischer@siemens-healthineers.com